Electronic Supplementary Information for: The slow Arrhenius process in small organic molecules

Federico Caporaletti* and Simone Napolitano*

E-mail: federico.caporaletti@ulb.be; simone.napolitano@ulb.be

Materials

The materials investigated, along with the parameters (activation energy and attempt frequency $\frac{1}{2\pi\tau_0}$) of the measured Slow Arrhenius Process are reported in Tab. 1.

Table S1: List of investigated materials, and properties of the corresponding SAP process: tris(4-carbazoyl-9-ylphenyl)amine (TCTA), bis(3-methylphenyl)-N,N'-diphenylbenzidine (TPD), telmisartan (TEL).

	T_g [K]	Manufacturer	E_{SAP} [kJ/mol]	$ln(f_0/\text{Hz})$
TCTA	423	Sigma-Aldrich	93 ± 3	27.2 ± 0.7
TPD	333	Sigma-Aldrich	97 ± 4	28.5 ± 1.1
TEL	409	Sigma-Aldrich	129 ± 4	39.16 ± 1.1

Dielectric spectra: experimental details

The complex capacitance of the samples was investigated in isothermal conditions for oscillating electric fields in the frequency range 0.1Hz$< f <$ 1 MHz, using an impedance analyzer (ModuLab XM MTS, Solartron Analytical). The dielectric spectra were then extracted from

the measurements of the capacitance, considering the relationship:

$$\epsilon(f) = \frac{C(f)d}{\epsilon_0 S} \tag{1}$$

where S and d are the nano-capacitor area and sample thickness respectively and $\epsilon_0 = 8.85 \times 10^{-12} Fm^{-1}$ is the vacuum permittivity.d was calculated from the capacitance measured at room temperature, in the parallel plate geometry approximation using

$$d = S\epsilon_\infty \epsilon_0 / C_\infty \, . \tag{2}$$

Here ϵ_∞ and C_∞ are the dielectric constant in absence of polarization processes ($T << T_g$). S was directly measured using optical microscopy: we found typical values of $5 \times 10^{-6}\mathrm{m}^2$. To quantitatively analyse the isothermal spectra, we described the frequency response of the samples considering three main contributions: i) the α-relaxation, modeled with an empirical Havrilak-Negami (HN) function,[1] ii) conductivity (σ) and the iii) SAP, modeled instead with a symmetric Cole-Cole function:

$$\epsilon(\omega) = \epsilon_\infty + \frac{\Delta\epsilon_\alpha}{[1 + (i\omega\tau_{HN})^{a_{HN}}]^{b_{HN}}} + \frac{\Delta\epsilon_{SAP}}{1 + (i\omega\tau)^{b_{SAP}}} + \frac{\sigma}{(i\omega\epsilon_0)^n} \, . \tag{3}$$

In Eq. 3 $\Delta\epsilon_\alpha$ is the dielectric strength associated to the α process, τ_{HN} is the HN time, a_{HN} and b_{HN} are the shape parameters associated to the width and asymmetry of the α-peak; σ is the conductivity and $n \leq 1$, $\Delta\epsilon_{SAP}$ is the dielectric strength of the SAP and $b_{SAP} \leq 1$ is the associated broadening parameter.[2] We found values of b_{SAP} close to 1, *i.e.*, $b_{SAP} \simeq 0.85 - 0.9$ for all the investigated molecules, meaning that the SAP has a shape close that of a single Debye relaxation process.

Dynamic calorimetry

The structural relaxation of TCTA could be probed by DS, we therefore extracted its characteristic timescale from fast calorimetry using a step-response analysis.[3–5] In more details,

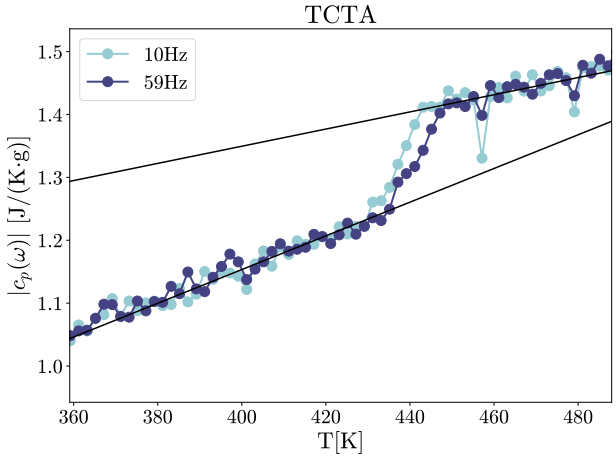

Figure S1: Modulus of the complex specific heat $c_p(\omega)$ of TCTA as a function of temperature at two different frequencies:10 and 59 Hz.

we accessed the atomic mobility across the glass transition by performing quick down-jumps (2000 K/s) in temperature followed by isotherms with different duration, namely 0.1024s and 0.0512s. This allowed us to measure the complex specific heat $c_p^*(\omega)$ with two different base frequencies, 10Hz and 20Hz respectively. $c_p^*(\omega)$ was calculated by performing the Fourier Transform of the instantaneous cooling rate ($q(t)$) and heat flow ($HF(t)$):[3–5]

$$c_p^*(\omega) = \frac{\int_0^{t_p} HF(t)e^{-i\omega t}dt}{\int_0^{t_p} q(t)e^{-i\omega t}dt} \tag{4}$$

where t_p is the oscillation period of the modulation. The α-relaxation is identified by the step in the modulus of the frequency dependent specific heat $|c_p(\omega)|$ (see Fig. S1)

Telmisartan

Fig. S2 shows the relaxation maps of telmisartan measured from a thin-film of 70nm using BDS. The black solid line shows the temperature dependence of the α-relaxation measured from a bulk sample obtained via physical vapour deposition.[6] .

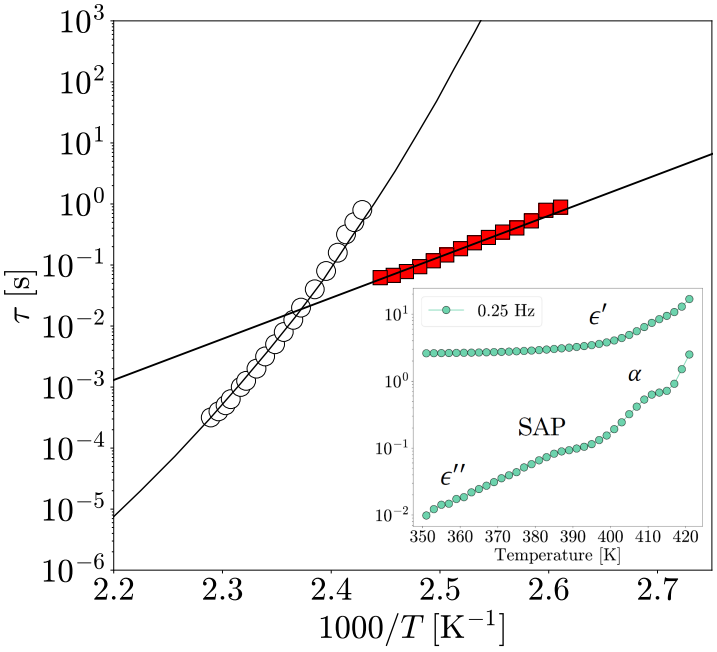

Figure S2: A: Relaxation map of telmisartan. White diamonds: α-relaxation as measured by dielectric spectroscopy. The black solid line shows the temperature dependence of the α-relaxation measured in a bulk sample.[6] Red squares: Slow Arrhenius process as measured by dielectric spectroscopy. B: Isochronal spectrum of the complex dielectric permittivity of telmisartan measured at 0.25 Hz.

3D spectra

Fig. S3 shows the 3-dimensional dielectric loss, as a function of temperature and frequency for TPD (A), TCTA(B) and TEL (C).

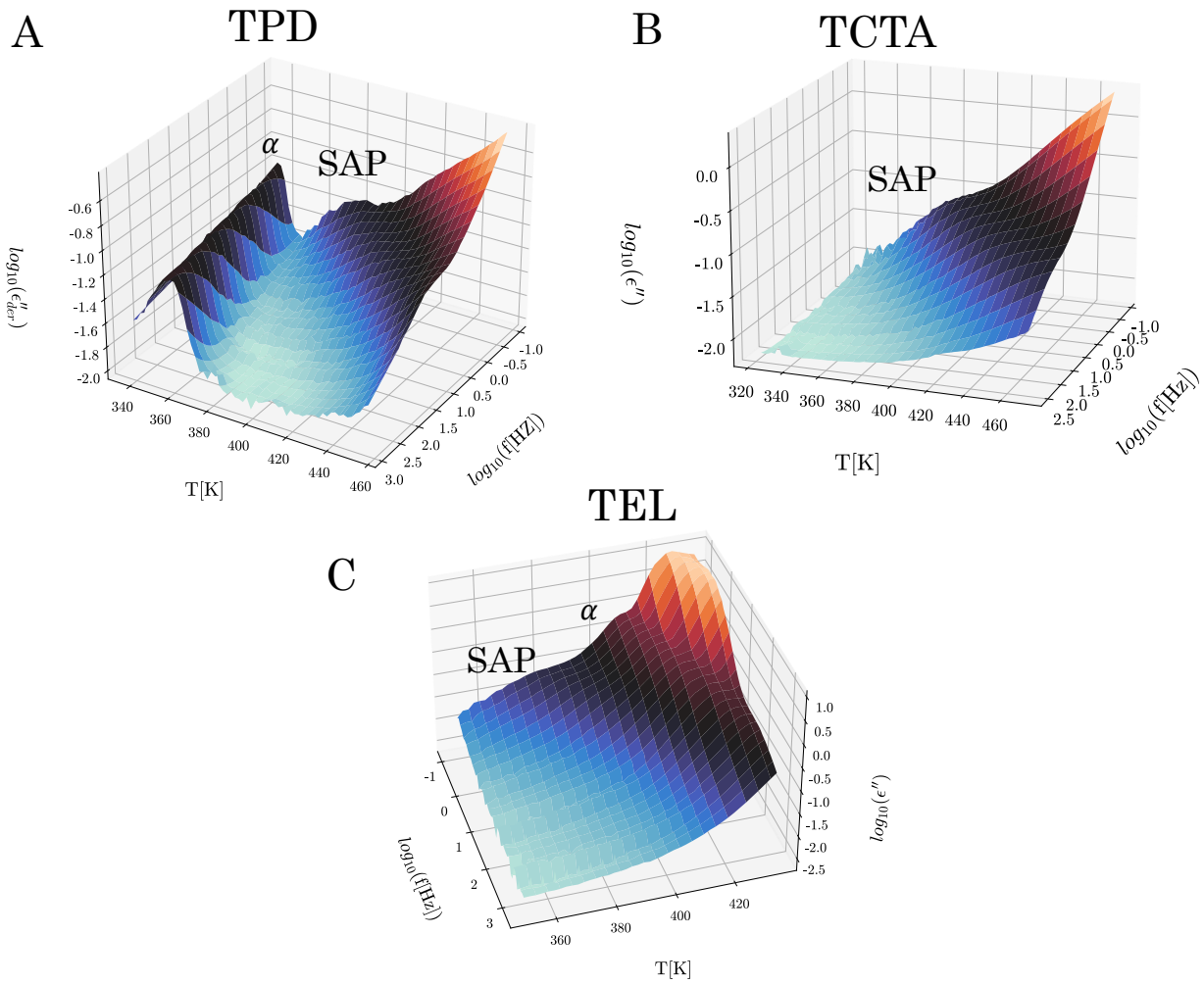

Figure S3: Examples of 3-dimensional plots of the dielectric loss, as a function of frequency and temperature, for films of TPD (A), TCTA (B) and TEL (C). In the case of TPD and TEL, to reduce the contribution of the conductivity, the dielectric loss is derived from the real part of the dielectric function, via the approximate relation $\epsilon''_{DER} = -\frac{\pi}{2}\frac{\partial\epsilon'}{\partial \ln\omega}$.[7]

Ethylcyclohexane

Fig. S4 reports the attempt rate (f_0) and the activation barrier (E_{SAP}) for the SAP-like process observed in Ref.[8] along with the values from the small molecules investigated in this work and polymers data from.[9]

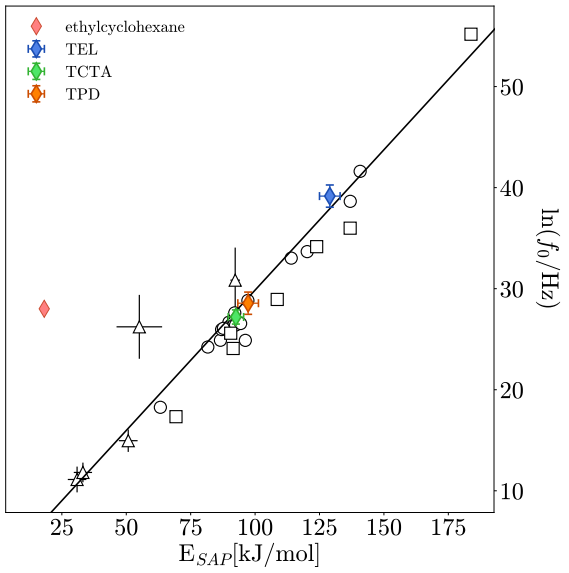

Figure S4: Correlation between the logarithm of the attempt rate (f_0) and the activation barrier (E_{SAP}) of the SAP of 31 polymeric systems (white circles) from Thoms and Napolitano;.[9] The same color code as Fig. S2-(b) is used. In addition to the small molecules here investigated, we report also the values for the Arrhenius process observed in ethylcyclohexane[8] (pink diamond). The values of attempt rate and activation barrier does not satify the enthalpy-entropy expected for the SAP.

References

(1) Kremer, F.; Schönhals, A. *Broadband dielectric spectroscopy*; Springer Science & Business Media, 2002.

(2) Song, Z.; Rodríguez-Tinoco, C.; Mathew, A.; Napolitano, S. Fast equilibration mechanisms in disordered materials mediated by slow liquid dynamics. *Science advances* **2022**, *8*, eabm7154.

(3) Shoifet, E.; Schulz, G.; Schick, C. Temperature modulated differential scanning calorimetry–extension to high and low frequencies. *Thermochimica Acta* **2015**, *603*, 227–236.

(4) Monnier, X.; Cangialosi, D. Thermodynamic ultrastability of a polymer glass confined at the micrometer length scale. *Physical Review Letters* **2018**, *121*, 137801.

(5) Di Lisio, V.; Gallino, I.; Riegler, S. S.; Frey, M.; Neuber, N.; Kumar, G.; Schroers, J.; Busch, R.; Cangialosi, D. Size-dependent vitrification in metallic glasses. *Nature Communications* **2023**, *14*, 40417.

(6) Rodríguez-Tinoco, C.; Ngai, K.; Rams-Baron, M.; Rodríguez-Viejo, J.; Paluch, M. Distinguishing different classes of secondary relaxations from vapour deposited ultrastable glasses. *Physical Chemistry Chemical Physics* **2018**, *20*, 21925–21933.

(7) Böttcher, C.; Bordewijk, P. Theory of electric polarization, vol. 2. 1978.

(8) Mandanici, A.; Huang, W.; Cutroni, M.; Richert, R. Dynamics of glass-forming liquids. XII. Dielectric study of primary and secondary relaxations in ethylcyclohexane. *The Journal of chemical physics* **2008**, *128*, 124505.

(9) Thoms, E.; Napolitano, S. Enthalpy-entropy compensation in the Slow Arrhenius Process. *The Journal of Chemical Physics* **2023**, *159*, 161103.